An International Journal of Optimization and Control: Theories & Applications
ISSN: 2146-0957 eISSN: 2146-5703
Vol. 16, No. 3, pp.1064-1085 (2026)
https://doi.org/10.36922/IJOCTA026090035

RESEARCH ARTICLE

Investigation of the elastic–plastic behavior of pipes and vertical risers in offshore hydraulic structures

Latif F. Aslanov[1,2†*] and Ulvi L. Aslanli[1,2†]

[1] OilGasScientificResearchProject" Institute, State Oil Company of the Azerbaijan Republic (SOCAR), Baku, Azerbaijan
[2] Azerbaijan University of Architecture and Construction, Baku, Azerbaijan
latif.aslanov@bk.ru; aslanliu@mail.ru

ARTICLE INFO

Article history:
Received: March 1, 2026
Revised: April 3, 2026
Accepted: April 8, 2026
Published Online: May 20, 2026

Keywords:
Standpipe
Offshore structures
Pipeline systems
Follower forces
Nonlinear theory

AMS Classification 2010:
90B23, 90B56

ABSTRACT

This article investigates the stability and strength of tubular elements in offshore oil and gas structures, considering internal fluid flow, centrifugal forces, and material nonlinearity. The main objective is to analyze the deformation of tubular elements under various fluid flow regimes and assess their stability under eccentricity and initial imperfections. Both elastic and elastoplastic material models are employed, along with the effects of distributed loads and axial forces. An increase in fluid flow velocity leads to significant changes in element behavior, reducing structural stability. The small parameter method is applied to capture nonlinear effects more accurately, providing analytical solutions for additional bending and their influence on structural stability. This approach allows for precise evaluation of tubular element behavior under internal fluid flow conditions and can be applied to the design, strength calculation, and optimization of pipelines and other hydraulic structures. Although fractional derivatives were not applied in this study, it is acknowledged that they have gained significant importance in modern research as powerful tools. These derivatives offer new analytical perspectives for modeling complex physical systems and have been increasingly used in various fields such as engineering, physics, and applied mathematics. The results contribute to practical engineering recommendations, operational improvement, and the design optimization of offshore infrastructure, ensuring applicability to a wide range of nonlinear structural mechanics problems.

1. Introduction

The installation of subsea pipelines is an essential component of modern oil and gas infrastructure and involves high-precision engineering operations. The activities carried out within a pipeline project consist of several stages, each aimed at ensuring the structural integrity, functionality, and safety of the pipeline. These stages include welding, insulation, installation of buoyancy modules and other technical equipment, transportation of the pipeline, offshore installation, and the performance of hydraulic testing.

After the completion of welding and insulation processes, the pipeline is equipped with head and end towing assemblies and is considered ready for transportation. The pipeline is positioned toward the shoreline using four pipe-laying lifting tractors, lowered onto the water surface, and then transported to the designated location by tugboats. Before the installation works begin, favorable weather conditions are forecasted—wave intensity up to 2 points and wind force up to 4

* Corresponding Author
† *These authors contributed equally to this work.*

points—and the operations are carried out with hydrographic and diving support.

During the positioning and securing of the pipeline, specialized equipment is used, including a 100-ton crane vessel and tugboats. Buoyancy systems are employed to bring the pipeline into its correct position, after which it is lowered to the seabed under its own weight. Once the laying process is completed, the pipeline is secured with clamps, and the section above the water level is stabilized.

Testing is carried out through hydraulic and gas tightness tests of the pipeline. These tests are performed in accordance with relevant standards to ensure the safe and reliable operation of the pipeline.

The implementation of these works requires careful selection of the pipeline route. The route is designed in areas where the seabed is relatively flat and uniform, ensuring the pipeline's long-term stability against wave and current forces during its operational life. The length of the pipeline specified in the project is determined based on assessments provided by specialists, considering the minimum allowable bending radii established for the onshore routing of the pipeline along the selected corridor.

This article reviews the engineering challenges encountered during the installation and testing of subsea pipelines, as well as the methodologies applied to address them. Using a pipeline project as an example, the importance of the methods and procedures employed at various stages—from determining the design length of the pipeline to ensure its proper installation—is emphasized.

The structural connection of vertical pipes to the stationary platform and deck elements, as well as their fastening to load-bearing legs, is illustrated in **Figures 1,2,3**, respectively. In this study, physically nonlinear analyses were carried out, considering the structural connection of the vertical pipes to the load-bearing legs of offshore hydraulic structures.

The effects of thermal processes on material degradation[1] have been investigated, friction resistance between buried coated steel pipes and soil[2] has been analyzed, and temperature effects on the load-bearing capacity of API X60 pipe elbows[3] have been modeled, demonstrating that thermomechanical factors can reduce pipeline operational reliability. In recent years, various methods for pipeline monitoring and fatigue life enhancement, including FSI-based multi-factor optimization approaches, have been applied.[4,5]

International and local studies have investigated the wave and dynamic interaction of large-section bored and CFA piles with soil,[6–8] examined the stress-strain state of piles and pontoon elements of fixed offshore platforms,[9–12] and addressed seismic effects on marine hydraulic structures and methods for increasing bearing capacity reserves.[13,14] In addition, foundations for reservoirs in the Caspian Sea and new calculation methods for pontoon elements of offshore fixed platforms have been developed,[15,16] as well as the local stability of sealed pipe elements and a methodology for calculating pile foundation load-bearing capacity based on rational design principles.[17,18]

In recent years, the dynamic and stress responses of pipelines have been investigated: the influence of impulse loads on fiberglass pipes has been studied using a vibroacoustic method,[19] turbulence modeling in pipe elbows under secondary flow conditions has been validated,[20] the effect of internal water on underground pipeline dynamics has been assessed,[21] nonlinear vibration analyses considering soft nonlinear clamps have been conducted,[22] nonlinear stress analysis of aero-engine pipelines using a semi-analytical method has been performed,[23] emerging hydroforming technologies and their parameters have been reviewed,[24] and the structural performance of fiber-reinforced patches for repairing damaged steel pipes has been experimentally evaluated.[25]

In recent years, the strength and dynamic behavior of underground and mechanical pipelines have been investigated: the multi-hole grouting repair of underground drainage pipeline defects has been studied numerically and experimentally,[26] the vibration behavior of viscoelastic cylindrical shells under internal moving pressure has been analyzed analytically,[27] the stress-strain model of austenitic stainless steel for pressure vessel design has been developed,[28] the dynamic response of reinforced soft tubes has been investigated numerically and experimentally,[29] random uncertainty modeling and vibration analysis of straight pipes conveying fluid have been conducted,[30] nonlinear forced vibration of porous functionally graded pipes in the subcritical regime has been evaluated,[31] and urban ground collapse induced by defective pipelines has been studied using physical model experiments and numerical simulation.[32]

Recent studies have investigated various aspects of pipeline systems and offshore structures: high-precision numerical modeling of projectile launch and failure mechanisms of structural components,[33] calculation of metal element deflection using a three-line strain diagram,[34] experimental and numerical analysis of failure in flexible pipes

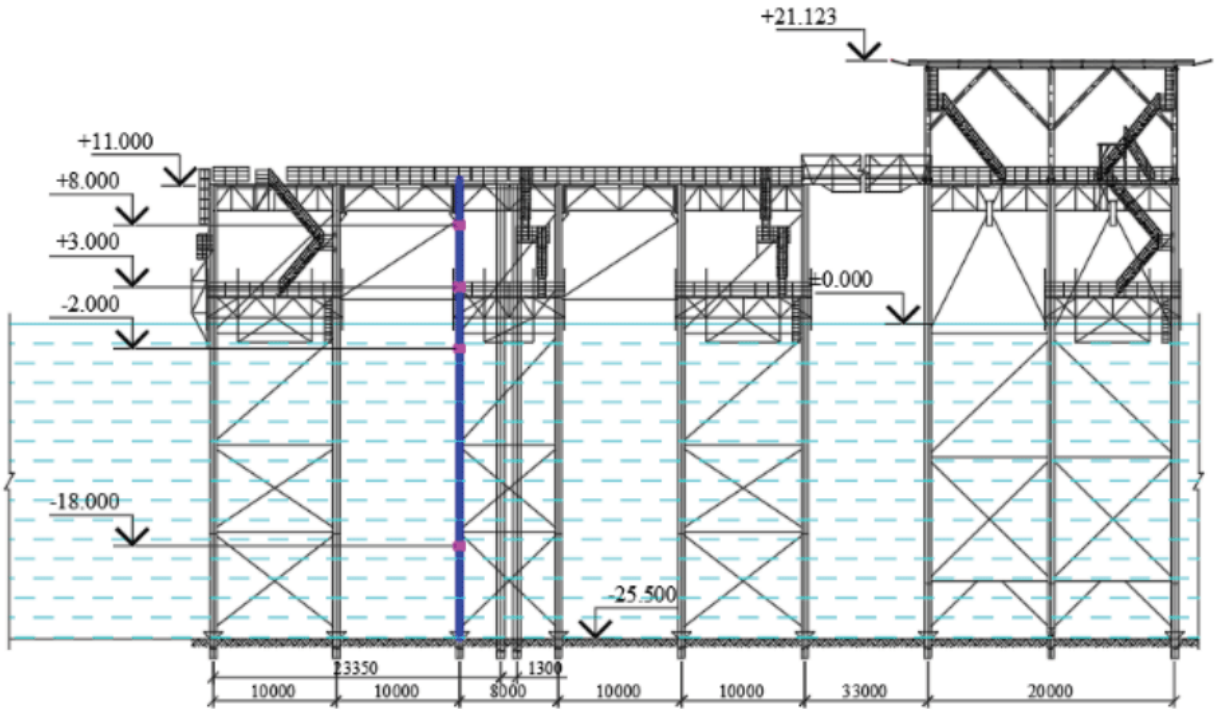

Figure 1. Installation, routing, and fastening of the vertical pipe from the seabed to the topside structure of the stationary offshore platform

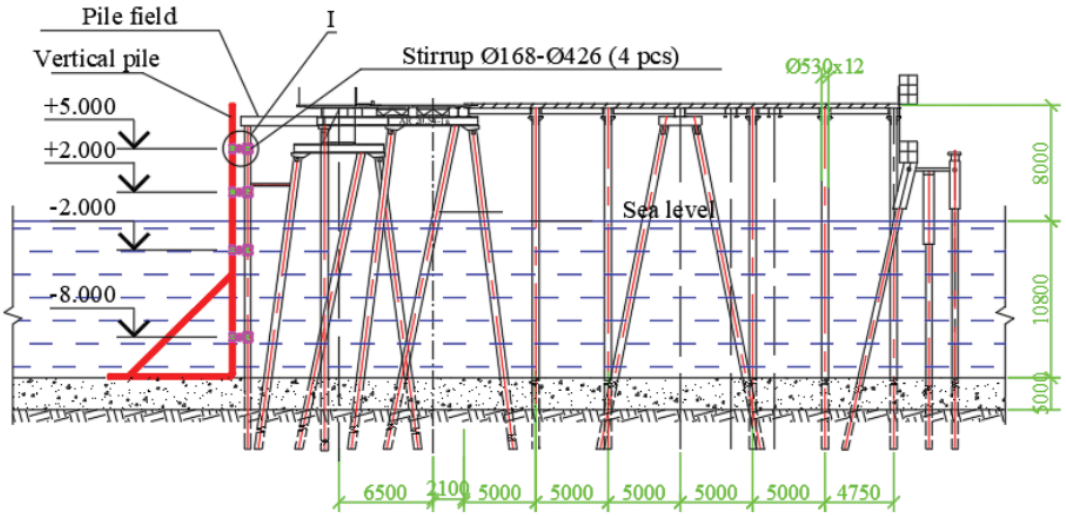

Figure 2. Installation, routing, and fastening of the vertical pipe from the seabed to the topside structure of the trestle-connected platform deck

due to intentional damage,[35] evaluation of submarine debris-flow hazard risks to planned subsea pipeline systems,[36] analysis of energy characteristic changes in pipeline systems under hydrodynamic loads,[37] study of structural changes in multifaceted gas pipelines,[38] vortex dynamics diagnosis in the stall state of mixed-flow pumps,[39] and the application of artificial intelligence for asset integrity management of offshore oil and gas pipelines.[40]

In recent years, studies on pipeline systems and related technological equipment have been conducted: the impact of pipe materials on water hammer in pressure pipelines has been studied experimentally and numerically,[41] a novel fractal fractional mathematical model for HIV/AIDS transmission stability and sensitivity with numerical analysis has been proposed,[42] the strength

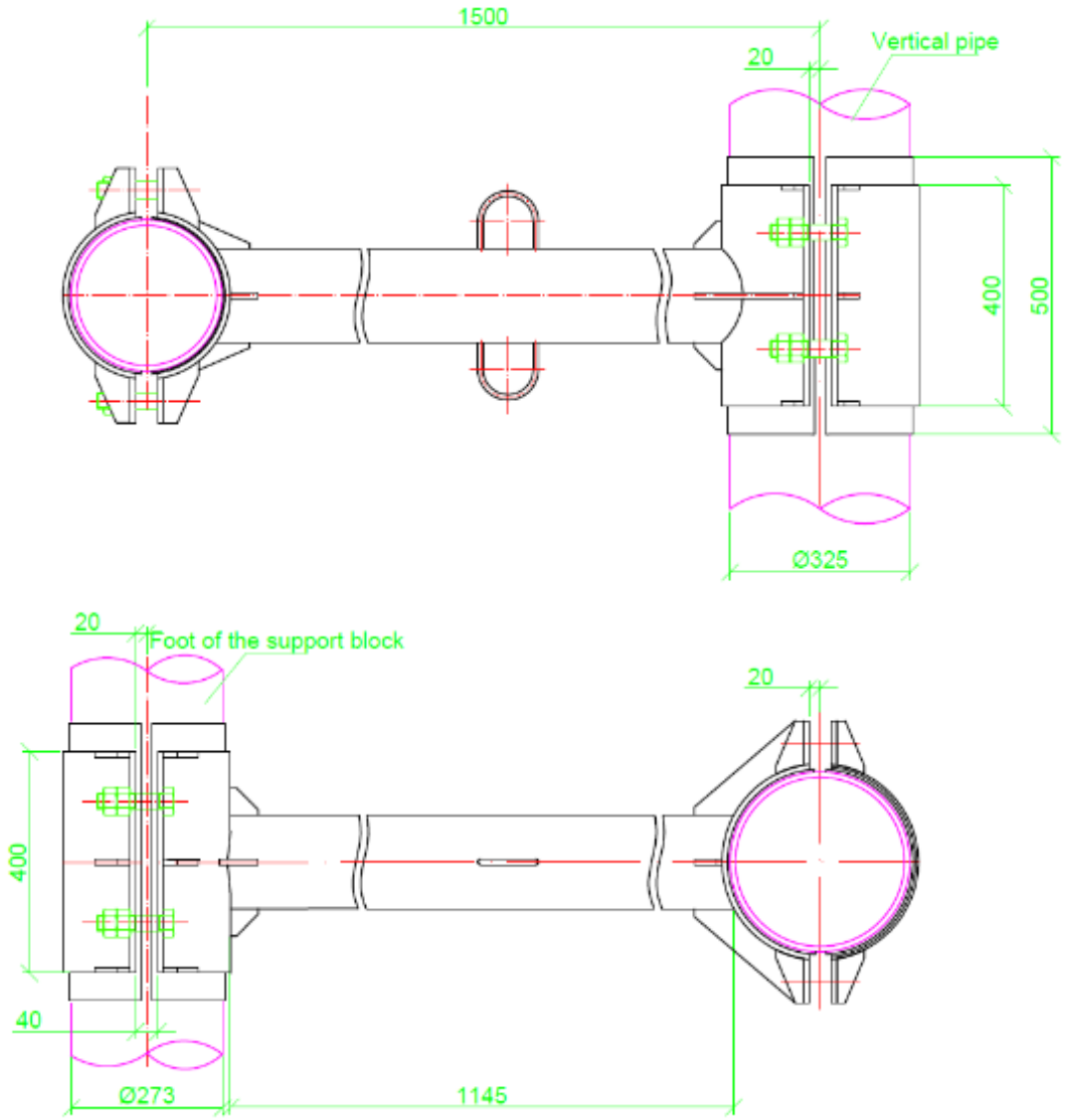

Figure 3. Schematic of the structural connection of the vertical pipe to the offshore hydraulic structure

of tanks filled with fluid under free drop conditions has been determined,[43] stability and nonlinear vibrations of closed cylindrical shells interacting with fluid flow have been reviewed,[44] prestressed concrete cylinder pipes reinforced with fiber-reinforced polymer have been analyzed,[45] shear effects on axisymmetric wave propagation in buried fluid-filled pipes have been evaluated,[46] effects of operation parameters on heat transfer in tubular moving bed heat exchangers have been investigated using CFD-DEM,[47] and the deformation behavior in tube hydro-pressing of rectangular cross-section components has been studied.[48]

In recent years, the dynamic, mechanical, and material behavior of pipeline systems has been investigated: in-plane and out-of-plane dynamics of curved pipes conveying fluid have been studied using the integral transform method,[49] throttle valve erosion in the oil and gas industry has been investigated,[50] vibration manipulation properties of phononic crystals and acoustic metamaterials for fluid-conveying pipeline systems have been reviewed,[51] the mechanism of post-buckling and initiation of a propagating buckle in sandwich pipelines has been studied based on shear deformation theory,[52] the influence of ductility on fracture in tensile testing of cold gas sprayed deposits has been evaluated,[53] flow properties of cemented paste backfill through L-pipe and loop-pipe tests have been experimentally investigated,[54] and bending vibration control of pipes conveying fluids has been studied using nonlinear torsional absorbers at the boundaries.[55]

In recent years, the material, mechanical, and operational characteristics of pipeline systems have been investigated: manufacturing defects in thermoplastic composite pipes and their in-

situ performance in oil and gas applications have been studied,[56] plant-derived extracts for mitigating scale formation in pipelines and industrial systems have been reviewed,[57] fluid-induced vibrations of long branched pipelines have been analyzed,[58] bending stresses in pipelines have been evaluated using hole-drilling measurements combined with interferometry,[59] the dynamic response of water in buried pipelines under explosion has been numerically simulated,[60] the viscosity of stabilized emulsions in different pipe diameters has been studied using pressure drop and phase inversion,[61] and buckling analysis of groove-corroded pipes under axial pressure has been performed using the finite element method.[62]

Recent studies have focused on pipeline systems and the effects of gas hydrates, soil, and fluid: the influence of bend diameter rate on the flow characteristics of natural gas hydrate particles in curved pipes has been numerically investigated,[63] deformable pipelines for efficient recovery of protective coal pillars have been designed,[64] and buckling and stability of subsea high-pressure/high-temperature pipelines on laterally sloping seabeds have been studied.[65] Additionally, the dynamics of materials recycling in chemostat systems have been analyzed with the help of an artificial deep neural network,[66] and deep neural networks have been applied in the computational analysis of coupled systems of fractional integro-differential equations.[67]

Other relevant work includes stress analysis of buried polyethylene pipes with viscoelastic behavior using the finite element method,[68] evaluation of the role of particulate shape and size in erosion of pipe bends via CFD,[69] and analysis of gas flow resistance in unstable collapse boreholes along with classification of borehole types.[70] Furthermore, neural network-based fixed-time tracking control methods for nonlinear systems with actuator faults have been developed,[71] and dynamic analysis of liquid-filled clamp-pipe systems has been carried out using the spectral element method.[72]

Recent studies have focused on pipeline dynamics, pipe-soil interaction, and corrosion issues: recent progress on dynamics and control of pipes conveying fluid has been reviewed,[73] a numerical study of pipe-soil interaction under lateral movements on different seabed types has been conducted,[74] and stress-strain rate curves of MR fluids and their application in sheet flexible-die forming have been investigated.[75] Additionally, progression of localized corrosion on inner walls of steel pipelines has been studied,[76] and internal erosion induced by infiltration of defective buried pipes has been experimentally and numerically investigated.[77]

Furthermore, pipe-soil interaction and sensitivity of large-diameter buried steel pipes have been analyzed,[78] and a theoretical analysis of deformation for steel gas pipes under surface explosion loads, considering shear effects, has been performed.[79] Corrosion inhibitors of API pipeline steels have been reviewed,[80] design pressure of in-service welding pipes has been studied,[81] and performance and stress analysis of flat-tubular solid oxide fuel cells fueled with methane and hydrogen has been investigated.[82]

Recent studies have focused on deep-water and offshore pipeline behavior, vibrations, and corrosion: research on buckling propagation experiments of deep-water pipelines has been conducted,[83] vortex-induced vibration suppression on subsea pipelines using helical strakes has been studied experimentally and numerically,[84] and mask privacy preservation prescribed-time consensus control for nonlinear multi-agent systems has been proposed.[85] Further investigations include the impact of structural parameters of multi-jointed pneumatic sealing discs in fluid-driven pipeline robots on performance,[86] fitness-for-service assessment of local thin areas in line pipes,[87] and tribo-corrosion behavior of oil country tubular goods.[88]

Other studies have addressed modal analysis of PE pipelines under seabed dynamic pressure,[89] damage mechanisms of offshore pipelines impacted by falling objects,[90] progress and prospects of particle finite element method for large deformation simulation in geotechnical engineering,[91] and stability and local bifurcation of parameter-excited vibration of pipes conveying pulsating fluid under thermal loading.[92]

Oil and gas pipelines and offshore structures are subjected to mechanical, thermal, hydrodynamic, and pipe-soil interaction effects,[1–92] yet the existing literature has not sufficiently addressed the additional bending induced by centrifugal or "follower forces" in standpipe-type elements conveying fluid. Furthermore, the combined influence of elastic and elastoplastic material models, initial imperfections, eccentricities, distributed loads, and axial forces remains largely unexplored. This study aims to evaluate the bending behavior and critical states of pipes and support elements under internal fluid flow using analytical and numerical approaches, filling a gap in current offshore and pipeline research.

1.1. Research innovations

This study introduces several innovative aspects in the analysis of tubular elements and vertical risers in offshore hydraulic structures:

Research perspective: The work addresses a gap in current offshore structural research by considering the combined effects of internal fluid flow, eccentricities, initial imperfections, and elastoplastic material behavior on the stability of pipes and risers. Unlike classical studies that focus primarily on linear or weakly nonlinear systems, this research provides a more realistic representation of operational conditions.

Analytical method: A novel combination of the elastoplastic constitutive model and the small parameter method is applied, allowing for precise evaluation of nonlinear deformations and stress-strain behavior. The approach offers improved predictive capability over classical Lyapunov stability analysis, particularly for systems experiencing significant material nonlinearity and large deformations.

Engineering applications: The proposed methodology facilitates practical optimization of geometric parameters and design recommendations for offshore structures. It can be directly applied to the design and analysis of marine risers, pipelines, and other tubular elements, enhancing both structural reliability and manufacturability.

By explicitly presenting these innovative points, the study clarifies its contribution from the research, analytical, and practical engineering perspectives, providing a clear framework for both current and future investigations in offshore structural analysis.

2. Materials and methods

This study investigates the behavior of vertical risers in marine hydraulic structures subjected to internal pressure. The primary objective was to develop a method for calculating and optimizing their geometric parameters while considering the material's physical nonlinearity, thereby addressing practical engineering challenges associated with offshore structures.

A general linearization approach was employed for thin-walled structures with variable geometric parameters, which facilitated the acceleration of convergence in the computational process. The computational method was based on the finite difference technique, implemented as a custom algorithm within an integrated software suite. The analysis was conducted within the framework of shell moment theory, enabling accurate assessment of structural behavior under complex loading conditions.

The proposed methodology explicitly incorporates the material's physical nonlinearity, allowing for precise evaluation of structural strength, deformation, and manufacturability. Calculations were performed on cylindrical shells with both constant and variable thicknesses, subjected to external loads and internal pressures under both axisymmetric and non-axisymmetric loading conditions. This ensures the applicability of the method to a wide range of real engineering scenarios.

All results were obtained through numerical simulations, and practical formulas and engineering recommendations were subsequently derived to support the design and analysis of marine hydraulic structures. The use of the finite difference method simplifies the calculation process by considering multiple levels of approximation, ultimately enabling the selection of optimal design solutions.

To justify the applicability of the proposed approach, it is important to compare it with classical stability analysis methods, such as Lyapunov stability theory. While Lyapunov-based approaches are effective for linear or weakly nonlinear systems, they are often limited in capturing complex material nonlinearity, geometric imperfections, and follower force effects in fluid-conveying tubular elements. In contrast, the present method explicitly incorporates elastoplastic behavior and nonlinear deformation effects, providing a more realistic representation of structural response under operational conditions. However, the proposed approach is mainly applicable to systems where material nonlinearity and large deformation effects are significant, whereas classical methods may remain more appropriate for purely elastic or simplified dynamic systems.

3. Results

3.1. Stability of a tubular element beyond the elastic limit under flowing fluid

In the practice of constructing offshore oilfield structures, in some cases, structures are used that serve as load-bearing elements while simultaneously providing transportation of petroleum products, technical water, and other fluids. For this purpose, the lower and upper chords of tubular trusses are employed. During operation, these trusses, in addition to the usual loads, also experience forces arising from the movement of fluid inside the pipes. The problem considered in this work has broad applications in various fields of engineering and relates to cases where follower forces are associated with the curvature of the

deformable system. If the axis of the member is straight, the member will remain in equilibrium at any fluid flow rate. It is now necessary to determine whether a curved equilibrium shape can exist, in which the bending of the member is induced by centrifugal forces of the fluid particles arising from the curvature of their trajectories. Such a phenomenon is natural, since when the member bends in one direction, the centrifugal forces are directed in the same direction, and the question is only whether the magnitude of these forces is sufficient to maintain the bend.

The type of problem under study was considered by the author for a member operating within the elastic range, in connection with the design of a special underwater pipeline. In that case, a loss of stability in the Euler sense was observed. As is known, in the classical stability problem of a column, its ideal vertical position is assumed. Due to this property of the model, the governing equation turned out to be homogeneous, and the displacement of the member's axis at the point of stability loss could be determined up to a single unknown parameter.

However, in practice, such systems often exhibit predefined deviations from ideal conditions, such as misalignment of the member's axis from the vertical, differences in support elevations, and similar imperfections. In such cases, the problem formulation differs significantly from the classical Euler problem. Deviations from the initial equilibrium shape occur under any, even very small, loads. In this situation, the governing equation becomes nonhomogeneous. It is no longer appropriate to speak of stability loss as branching of equilibrium forms, and the "bifurcation" criterion becomes inapplicable. Considering the problem in the presence of imperfections demonstrates that critical states still exist, but of a different nature than in the idealized formulation.

Let us consider a pipe of length l, subjected to a uniformly distributed load $q_0$along its length and an axial force N, through which a fluid flows with velocity V. The upper end of the pipe rests on a horizontally compliant support. Moments $M_0$and $M_1$are applied at the ends of the pipe (**Figure 4**).

We apply the following sign convention: the axis of the member points to the right, the x-axis points downward, and placing the origin at the center of the pipe's upper support, the bending moment $M_x$is considered positive when acting clockwise, and the shear force $Q_x$is considered positive when acting to the right. Due to the presence of the upper compliant support, there is an initial deflection y_0. The liquid will flow through the pipe if the pressure difference at the ends of the pipe is not zero. This can be ensured if the pressure at the upper end at the pipe inlet is properly defined.

$$P_b = P_0 - \rho\frac{\vartheta^2}{2}, \tag{1}$$

At the lower end (outlet), the pressure is

$$P_n = P_0 + \rho\frac{\vartheta^2}{2} \tag{2}$$

That is, fluid is drawn into the upper end of the pipe, which is possible only if the pressure there is lower than the pressure in the surrounding liquid environment, while at the lower end, outflow occurs under a high external pressure corresponding to the dynamic head; otherwise, the fluid cannot exit from the lower end. In this case, the pressure difference will be:

$$P = P_n - P_v = P_0 + \rho\frac{v^2}{2} - \left(P_0 - \rho\frac{v^2}{2}\right) = \rho v^2, \tag{3}$$

In other words, the pressure difference is equal to twice the dynamic head.

Since the fluid flows through a pipe with a cross-sectional area of F_n, the dynamic head will be:

$$P_{sk} = F_n\rho v^2 = \frac{qv^2}{g} \tag{4}$$

where $q$is the weight of the fluid per unit length of the pipe;

is the acceleration due to gravity.

The bending moment $M_x$at an arbitrary section, based on **Figure 4**, can be expressed as:

$$M_x = M_0 + Q_0 x + q_0\frac{x^2}{2} - N\,(y - y_0) - \frac{qv^2}{g}(y - y_0). \tag{5}$$

Using the approximate differential equation of the curved axis of the rod

$$y'' = \frac{M_x}{EJ} \tag{6}$$

and by differentiating it twice, we obtain:

$$y^{IY} + \frac{1}{EJ}\left(N + \frac{qv^2}{g}\right)y'' = \frac{q_0}{EJ}. \tag{7}$$

Here, $\frac{qv^2}{g}y''$represents the intensity of the distributed inertial load.

Thus, the transverse load on the pipe, arising due to the flow of fluid through the pipe, "follows" the second derivative of the function describing the deflection of the pipe axis, and the intensity of this load depends on the fluid flow velocity ϑ.

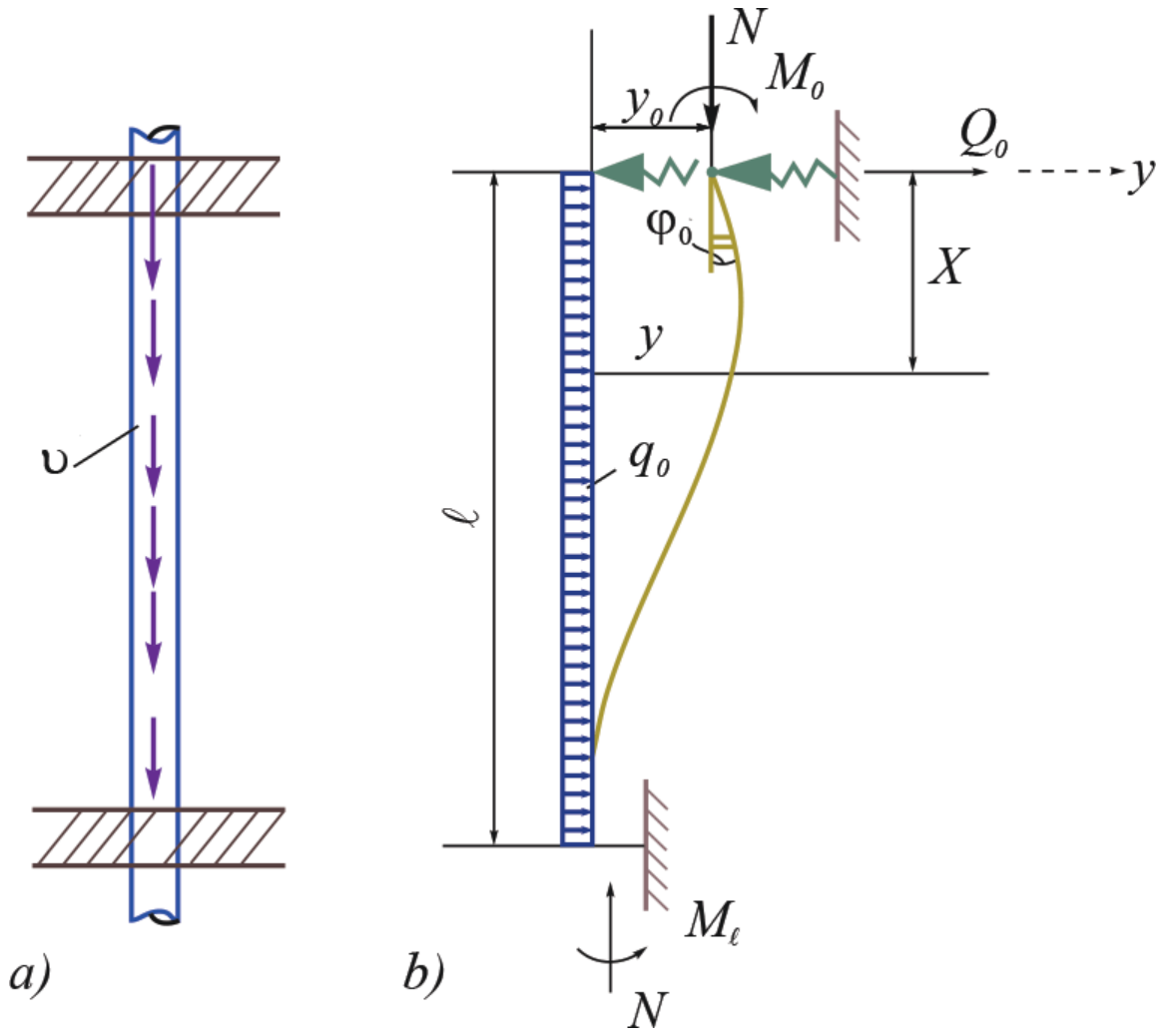

Figure 4. Schematic diagram of the loading condition of a pipe element

Finding the general solution of **Equation 7** does not present any fundamental difficulties.

Equation 7 characterizes the behavior of the tubular rod within the elastic range.

If we want to account for the behavior of the rod beyond the elastic range, it is necessary to use the following approximate form of the differential bending equation:

$$y'' = -\frac{\sigma_a}{Ec} \tag{8}$$

Here, $\sigma_a$and $E$are the yield stress and the modulus of elasticity of the rod material, and $c$is the height of the compressed zone of the elastic core.

To solve the stability problem of a tubular rod considering the elastoplastic properties of the material, we examine a simplified loading scheme; that is, a tubular rod supported on two supports, compressed by a longitudinal force $N$with an eccentricity e_0, and subjected to the inertial load $(qv^2)/g$. It is assumed that local buckling of the pipe wall is ensured. Under this loading scheme, the magnitude of the maximum bending moment will be:

$$M = \left(N + \frac{qv^2}{g}\right)(e_0 + y_0)\,, \tag{9}$$

Here, $y_0$is the maximum deflection at midspan.In this case, we use the approximate expression for the curved axis of the rod in the form:

$$y = y_0 \sin\frac{\pi x}{l} \tag{10}$$

For the section of the rod at midspan, at $x = l/2$, using **Equation 8**, we obtain the relationship

$$l^2 = \frac{\pi^2 E}{\sigma_a} y_0 c, \tag{11}$$

which characterizes the equilibrium states of the rod under axial stress $\sigma_0 = N/F$. Here, $F$is the cross-sectional area of the tubular rod.

We assume that the section exhibits one-sided yielding. The stress distribution for the midsection of the rod under one-sided yielding is shown in **Figure 5**. As the current coordinate, we take the central angle α, measured from the vertically downward radius. The boundary between

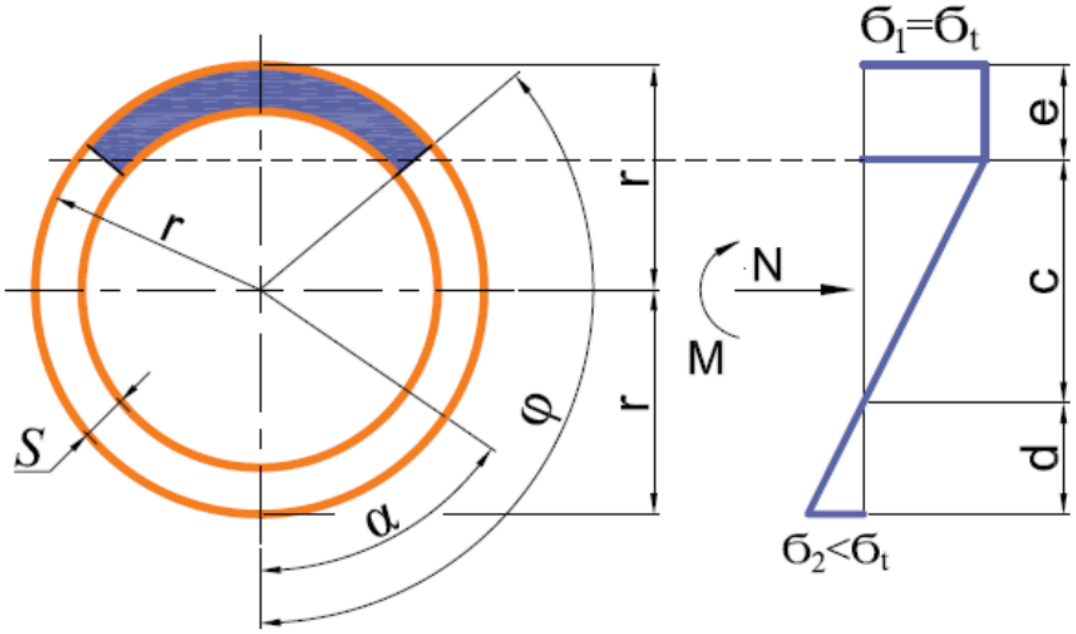

Figure 5. Midsection stress under one-sided yielding

the elastic core and the plastic zone is characterized by the central angle φ, and the maximum fiber stresses in the midsection of the rod are: on the concave side $\sigma_1 = \sigma_a$, and on the convex side $\sigma_2 < \sigma_a$.

The equilibrium condition for the tubular section, based on **Figure 5**, will have the form:

$$N = 2\pi r\delta\sigma_0 = 2\pi r\delta\sigma_a - 2r\delta\frac{\sigma_2 - \sigma_1}{1-\cos\varphi}$$

$$\int_0^{\varphi}(\cos\alpha\ -\cos\varphi\ )d\alpha = 2r\delta$$

$$\times\left[\pi\sigma_a - \frac{\sin\varphi - \varphi\cos\varphi}{1-\cos\varphi}(\sigma_2+\sigma_a)\right]; \quad (12)$$

$$M = \left(N + \frac{qv^2}{g}\right)(e_0 + y_0) = 2r^2\delta\frac{\sigma_2-\sigma_1}{1-\cos\varphi}$$

$$\times\int_0^{\varphi}\cos\alpha\ (\cos\alpha\ -\cos\varphi\ )d\alpha$$

$$= r^2\delta\frac{\varphi - \sin\varphi\cos\varphi}{1-\cos\varphi}(\sigma_2+\sigma_a); \quad (13)$$

Eliminating $\sigma_2$from these equations, we obtain

$$\frac{y_0}{r} = \frac{\sigma_a - \sigma_0}{2\left(\sigma_0 + \frac{qv^2}{g}\right)}\frac{\varphi - \sin\varphi\cos\varphi}{\sin\varphi - \varphi\cos\varphi} - \frac{e_0F}{2w} \quad (14)$$

Here, $w$is the section modulus of the tubular section, and the distance $c$from the neutral axis of the stress distribution to the boundary of the elastic core is given by:

$$\frac{\mathrm{c}}{r} = \frac{1}{\pi}\frac{\sigma_a}{\sigma_a - \sigma_0}(\sin\varphi - \varphi\cos\varphi\ ). \quad (15)$$

Therefore, based on 11 and considering expressions 14 and 15, we obtain the formula for the flexibility of the tubular rod in the equilibrium state:

$$\frac{l^2}{r^2} = \lambda^2 = \frac{\pi E\phi}{2\left(\sigma_0 + \frac{q\vartheta^2}{gF}\right)}, \quad (16)$$

where the following are denoted:

$$\phi = \varphi - \sin\varphi\cos\varphi - \frac{\sigma_0 gF + q\vartheta^2}{(\sigma_a - \sigma_0)\,g}$$

$$\bullet\frac{e_0}{w}(\sin\varphi - \varphi\cos\varphi\ ). \quad (17)$$

Stability (or Buckling) loss criterion:

$$\frac{d\phi}{d\alpha} = 0 \quad (18)$$

allows one to determine

$$\sigma_0 = \frac{\sigma_a - \frac{qv^2}{2g}\bullet\frac{e_0}{w}\frac{\varphi}{\sin\varphi}}{1 + \frac{e_0F}{2w}\frac{\varphi}{\sin\varphi}} \quad (19)$$

We have considered a section with one-sided yielding. Now we move on to the consideration of a section with two-sided yielding **Figure 6**. Retaining the previously adopted angle reference, we denote by $\phi$and $\psi$the angles that define the boundaries of the elastic core at the points adjoining

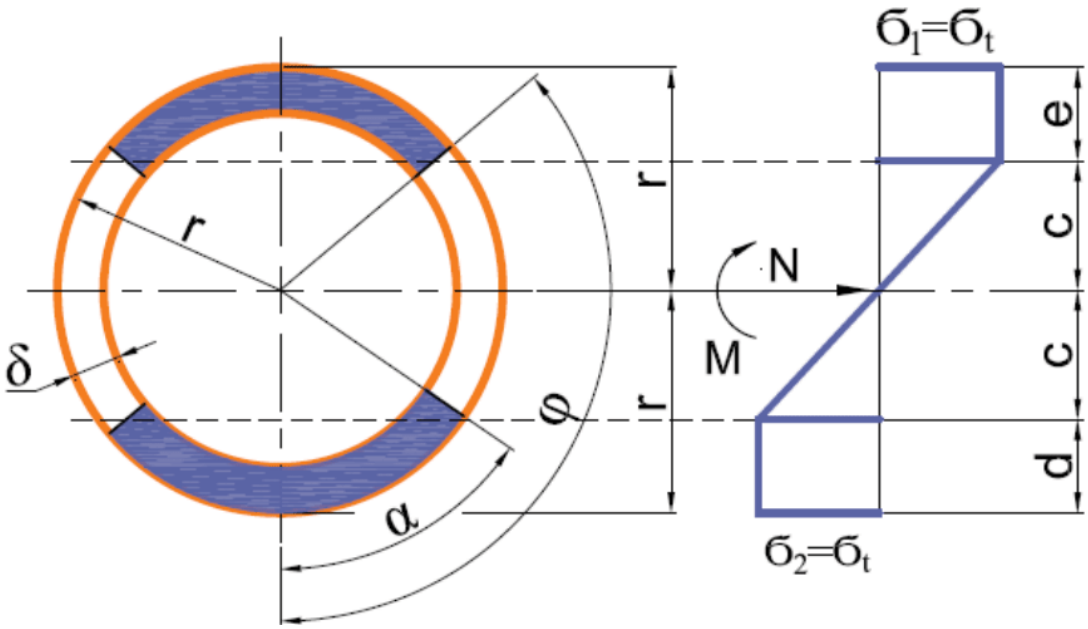

Figure 6. Midsection stress under two-sided yielding

the zones of plastic compression and, respectively, tension.

The equilibrium condition for the tubular section, based on **Figure 6**, will be:

$$N = 2\pi r\delta\sigma_0 = 2\pi r\delta\sigma_1(\pi - 2\psi) - \frac{4r\delta\sigma_a}{\cos\psi - \cos\varphi} \times \int_{\psi}^{\varphi}(\cos\alpha - \cos\psi)\,d\alpha = 4r\delta\sigma_a \left[\frac{\pi}{2} - \frac{(\sin\varphi - \varphi\cos\varphi) - (\sin\psi - \psi\cos\psi)}{\cos\psi - \cos\varphi}\right] \tag{20}$$

$$M = \left(N + \frac{q\vartheta^2}{g}\right)e_0 + y_0 = 4r^2\delta\sigma_a \left[\int_0^{\varphi}\cos\alpha d\alpha + \frac{1}{\cos\psi - \cos\varphi}\int_{\psi}^{\varphi}\cos\alpha(\cos\alpha - \cos\psi)\,d\alpha\right] = 2r^2\delta\sigma_a \frac{(\varphi - \sin\varphi\cos\varphi) - (\varphi - \sin\psi\cos\psi)}{\cos\psi - \cos\varphi} \tag{21}$$

From Equation 21, we find:

$$\frac{y_0}{r} = \frac{\sigma_a}{\sigma_0 + \frac{q\vartheta^2}{gF}} \bullet \frac{1}{\pi}\frac{(\varphi - \sin\varphi\cos\varphi) - (\psi - \sin\psi\cos\psi)}{\cos\psi - \cos\varphi} - \frac{e_0 F}{2w} \tag{22}$$

The distance c from the zero point of the stress diagram to the boundary of the elastic core is equal to:

$$\frac{c}{r} = \frac{\cos\psi - \cos\varphi}{2} \tag{23}$$

Consequently, based on 5 and considering expressions 16 and 17, we obtain the flexibility formula for the tubular rod in the equilibrium state:

$$\lambda^2 = \frac{\pi E\psi}{2\left(\sigma_0 + \frac{q\vartheta^2}{gF}\right)}, \tag{24}$$

where it is denoted:

$$\psi(\varphi,\psi) = (\varphi - \sin\varphi\cos\varphi) - (\varphi - \sin\psi\cos\psi) - \frac{\sigma_0 gF + qv^2}{2g\sigma_a}\frac{e_0}{w}\pi(\cos\psi - \cos\varphi). \tag{25}$$

The stability analysis problem is reduced to finding the function of two variables $\Psi(\phi,\psi)$under the additional condition:

$$\Theta(\varphi,\psi) = \frac{(\sin\varphi - \varphi\cos\varphi) - (\sin\psi - \psi\cos\psi)}{\cos\psi - \cos\varphi} = \frac{\pi}{2}\frac{\sigma_a - \sigma_0}{\sigma_a}, \tag{26}$$

which follows from 20.

We obtain an equation that relates the angles φ and ψ in the critical state of the rod.

$$\left[\frac{\pi}{2}\left(\cos\psi\ -\cos\varphi\ \right)+\left(\sin\psi\ -\psi\cos\psi\ \right)\right.$$
$$-\left(\sin\varphi\ -\varphi\cos\varphi\ \right)\frac{e_0F}{2w}=\sin\psi$$
$$\left.\cos\psi-\sin\varphi\cos\varphi+\frac{\left(\sin\varphi-\sin\psi\ \right)^2}{\varphi-\psi}\right] \quad (27)$$

Based on Equation 21, we obtain

$$\sigma_0=\frac{\sigma_a}{(e_0+y_0)}$$
$$\bullet\frac{r}{\pi}\frac{\left(\varphi-\sin\varphi\ \cos\varphi\ \right)-\left(\psi-\sin\psi\ \cos\psi\ \right)}{\cos\psi\ -\cos\varphi}-\frac{q\vartheta^2}{gF}. \quad (28)$$

As can be seen from expressions 19 and 28, the magnitude of the critical stress or axial force depends on the square of the velocity of the fluid flowing through the pipe. The higher the fluid velocity, the lower the allowable stress on the pipe body.

3.2. Analysis of the stress–strain state of a vertical riser in oil and gas production structures

A thin-walled vertical pipe is strongly affected by internal pressure (**Figure 7**). To analyze the stress state of such a pipe, the main equations of the moment theory for rotational shells symmetrically loaded along the axis can be applied.

$$\begin{cases} T_x=\dfrac{Eh}{1-\mu^2}\left(\dfrac{du}{dx}+\mu\dfrac{\omega}{r}\right) \\ T_t=\dfrac{Eh}{1-\mu^2}\left(\dfrac{\omega}{r}+\mu\dfrac{du}{dx}\right) \\ M_x=D\dfrac{d^2\omega}{dx^2} \\ M_t=\mu D\dfrac{d^2\omega}{dx^2} \end{cases} \quad (29)$$

In **Equation** 29, T_x, T_t – are normal forces in the shell's cross sections; r, h, z – is a current coordinate; P_1, P_2 – are the meridian, tangential projections of the given plane forces normal to the plane; u, w – are the displacement projections; E, β, μ – are elastic constants of material; ϵ_x, ϵ_y – are relative and anglular deformastions, $D=\frac{Eh^3}{12(1-\mu^2)}$ – flexural rigidity of the pontoon.

Taking the dependence between stress and strain as $\sigma=\varepsilon E-\beta\varepsilon^3$, we accept the physical equations as follows:

$$E\varepsilon_x-\beta\varepsilon_x^3=\sigma_x-\mu\sigma_y; E\varepsilon_y-\beta\varepsilon_y^3=\sigma_y-\mu\sigma_x \quad (30)$$

If we find σ_x, σ_y from **Equations** 30 and consider them in their nonlinear dependence between stress and strain

$$\sigma_x=\frac{4}{3}\left\{E\left(\frac{\partial u}{\partial x}+\frac{\partial^2 w}{\partial x^2}z+\frac{1}{2}\frac{w}{r}\right)\right.$$
$$\left.-\beta\left[\left(\frac{\partial u}{\partial x}+\frac{\partial^2 w}{\partial x^2}z\right)^3+\frac{1}{2}\left(\frac{\omega}{r}\right)^3\right]\right\}$$
$$\sigma_y=\frac{4}{3}\left\{E\left(\frac{w}{r}+\frac{1}{2}\left(\frac{\partial u}{\partial x}+\frac{\partial^2 w}{\partial x^2}z\right)\right)\right.$$
$$\left.-\beta\left[\left(\frac{\omega}{r}\right)^3+\frac{1}{2}\left(\frac{\partial u}{\partial x}+\frac{\partial^2 w}{\partial x^2}z\right)^3\right]\right\} \quad (31)$$

Considering the physical nonlinearity of the material and loading, it is necessary to solve the system of nonlinear differential equations for studying the case of deformation under tension. To solve such a complex task, we use the method of small parameters. For this, we take a small parameter as follows: $\nu=\frac{\beta\varepsilon_0^2}{E}$, here: ε_0 is the relative linear deformation corresponding to the strength limit. The solution of the system of **Equations** 29 is sought in the form of the following series with small parameters. Here: ϵ_0, γ_0 are relative and angular deformations corresponding to ultimate strength. It is seen from this expression that at the assumption of incompressibility of nonlinear materials.

$$u=\sum_{j=0}u_j\nu^j; w=\sum_{j=0}w_j\nu^j,\ \text{there}\ (j=0,1,2\ldots) \quad (32)$$

We substitute the series 32 in 29 taking this into account, we get the following system of linear equations:

for j=0,

$$\begin{cases} T_{x_0}=\dfrac{4}{3}Eh\left(\dfrac{\partial u_0}{\partial x}+\dfrac{\omega_0}{2r}\right) \\ T_{t_0}=\dfrac{4}{3}Eh\left(\dfrac{\omega_0}{r}+\dfrac{1}{2}\cdot\dfrac{\partial u_0}{\partial x}\right) \\ M_{x_0}=\dfrac{Eh^3}{9}\cdot\dfrac{d^2\omega_0}{dx^2} \\ M_{t_0}=\dfrac{Eh^3}{18}\cdot\dfrac{d^2\omega_0}{dx^2} \end{cases} \quad (33)$$

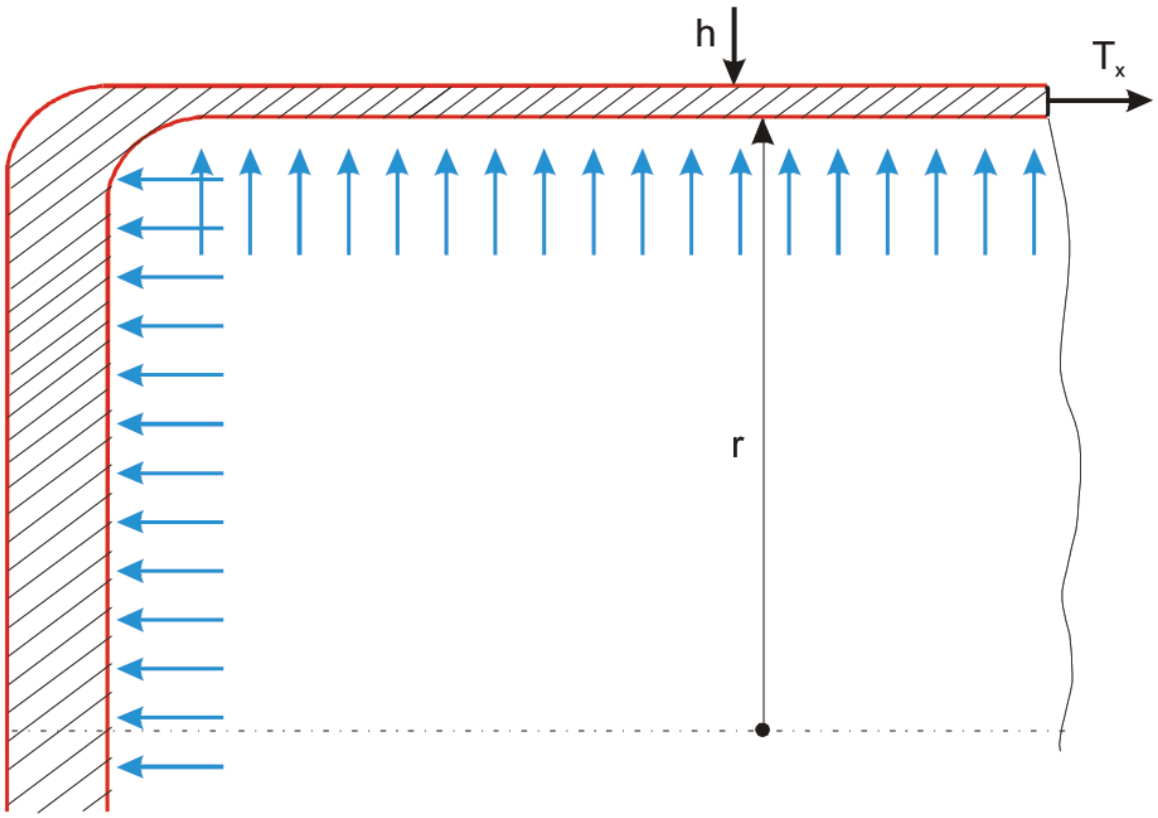

Figure 7. Structure and load calculation diagram of a thin-walled vertical pipe

for j=1,

$$T_{x_1} = \frac{4}{3}Eh\left\{\frac{du_1}{dx} + \frac{1}{2}\cdot\frac{\omega}{r} - \frac{1}{\varepsilon_0^2}\left[\frac{1}{2}\left(\frac{\omega_0}{r}\right)^3 + \left(\frac{du_0}{dx}\right)^3 + \frac{h^2}{4}\cdot\frac{du_0}{dx}\left(\frac{d^2w_0}{dx^2}\right)^2\right]\right\}$$

$$T_{t_1} = \frac{4}{3}Eh\left\{\frac{\omega_1}{r} + \frac{1}{2}\cdot\frac{du_1}{dx} - \frac{1}{\varepsilon_0^2}\left[\left(\frac{\omega_0}{r}\right)^3 + \frac{1}{2}\left(\frac{du_0}{dx}\right)^3 + \frac{h^2}{8}\cdot\frac{du_0}{dx}\left(\frac{d^2w_0}{dx^2}\right)\right]\right\}$$

$$M_{x_1} = \frac{Eh^3}{9}\left\{\frac{d^2w_1}{dx^2} - \frac{3}{\varepsilon_0^2}\left[\left(\frac{du_0}{dx}\right)^2\cdot\frac{d^2w_0}{dx^2} + \frac{h^2}{20}\cdot\left(\frac{d^2w_0}{dx^2}\right)\right]\right\}$$

$$M_{t1} = \frac{Eh^3}{9}\left\{\frac{1}{2}\frac{d^2w_1}{dx^2} - \frac{3}{2\varepsilon_0^2}\left[\left(\frac{du_0}{dx}\right)^2\cdot\frac{d^2w_0}{dx^2} + \frac{h^2}{20}\cdot\left(\frac{d^2w_0}{dx^2}\right)^3\right]\right\} \quad (34)$$

for j=2,

$$T_{x_2} = \frac{4}{3}Eh\left\{\frac{du_2}{dx} + \frac{1}{2}\cdot\frac{\omega}{r} - \frac{1}{\varepsilon_0^2}\left[\frac{3}{2r^3}\omega_0^2\omega_1 + 3\left(\frac{du_0}{dx}\right)^2\frac{du_1}{dx} + \frac{h^2}{4}\cdot\frac{du_1}{dx}\left(\frac{d^2w_0}{dx^2}\right)^2 + \frac{h^2}{2}\cdot\frac{du_0}{dx}\cdot\frac{d^2w_0}{dx^2}\cdot\frac{d^2w_1}{dx^2}\right]\right\}$$

$$T_{t_2} = \frac{4}{3}Eh\left\{\frac{w_2}{r} + \frac{1}{2}\frac{du_2}{dx} - \frac{1}{\varepsilon_0^2}\left[\frac{3}{r^3}\omega_0^2\omega_1 + \frac{3}{2}\left(\frac{du_0}{dx}\right)^2\frac{du_1}{dx} + \frac{h^2}{8}\cdot\frac{du_1}{dx}\left(\frac{d^2w_0}{dx^2}\right)^2 + \frac{h^2}{4}\cdot\frac{du_0}{dx}\cdot\frac{d^2w_0}{dx^2}\cdot\frac{d^2w_1}{dx^2}\right]\right\}$$

$$M_{x_2} = \frac{Eh^3}{9}\left\{\frac{d^2w_2}{dx^2} - \frac{3}{\varepsilon_0^2}\left[2\cdot\frac{du_0}{dx}\cdot\frac{du_1}{dx}\cdot\frac{d^2w_0}{dx^2} + \left(\frac{du_0}{dx}\right)^2\frac{d^2w_1}{dx^2} + \frac{3h^2}{20}\cdot\left(\frac{d^2w_0}{dx^2}\right)^2\cdot\frac{d^2w_1}{dx^2}\right]\right\}$$

$$M_{t_2} = \frac{Eh^3}{9}\left\{\frac{1}{2}\cdot\frac{d^2w_2}{dx^2} - \frac{3}{\varepsilon_0^2}\left[\frac{du_0}{dx}\cdot\frac{du_1}{dx}\cdot\frac{d^2w_0}{dx^2} + \left(\frac{du_0}{dx}\right)^2\frac{d^2w_1}{dx^2} + \frac{3h^2}{20}\cdot\left(\frac{d^2w_0}{dx^2}\right)^2\cdot\frac{d^2w_1}{dx^2}\right]\right\} \quad (35)$$

If we consider the system of **Equations**(33-35) in equilibrium equations $dQ/dx + T_t/r = P_1$;

$\frac{dT_x}{dx} = P_2$; $\frac{dM_x}{dx} = Q$, we get the following system of linear differential equations:

$$\frac{d^4\omega_0}{dx^4} + 4\beta^4\omega_0 = -\frac{1}{2}\cdot\frac{T_{x_0}}{rD} + \frac{P_1}{D}$$

$$\frac{d^4\omega_1}{dx^4} + 4\beta^4\omega_1 = \frac{3}{\varepsilon_0^2}\cdot\frac{d^2}{dx^2}\left[\left(\frac{3}{4}\cdot\frac{T_{x_0}}{Eh}\cdot\frac{1}{2}\cdot\frac{\omega_0}{r}\right)^2 \cdot\frac{d^2w_0}{dx^2} + \frac{h^2}{20}\cdot\left(\frac{d^2w_0}{dx^2}\right)^3 + \frac{9}{r^4h^2\varepsilon_0^2}\omega_0^3\right] \tag{36}$$

$$\frac{d^4\omega_2}{dx^4} + 4\beta^4\omega_2 = \frac{27}{\varepsilon_0^2 r^4 h^2}\omega_0^2\omega_1 + \frac{3}{\varepsilon_0^2}\cdot\frac{d^2}{dx^2} \times \left[2\frac{du_0}{dx}\cdot\frac{du_1}{dx}\cdot\frac{d^2w_0}{dx^2} + \left(\frac{du_0}{dx}\right)^2\frac{d^2w_1}{dx^2} + \frac{3h^2}{20}\cdot\left(\frac{d^2w_0}{dx^2}\right)^2\cdot\frac{d^2w_1}{dx^2}\right]$$

The physical nonlinearity and the variation in the geometric parameters of the elements were taken into account while performing complex calculations and optimizations for the pipe and vertical riser (riser) elements used in offshore hydraulic structures. Analytical solutions were obtained for vertical pipe elements. The mechanical behavior of the structures was assessed under various loading conditions, considering both external and internal pressure effects. The application of the physical nonlinear theory allowed for a more accurate determination of the stress and strain fields, revealing additional strength reserves of the material. Generalized equations and engineering recommendations were developed for optimizing the dimensions of structural elements, resulting in enhanced load-bearing capacity, structural efficiency, and manufacturing technological feasibility. Overall, the results demonstrate the potential application of the proposed methodology in nonlinear structural mechanics. A graphical representation of the dimensionless stress-strain relationship is provided in the Graphical Abstract.

A methodology for calculation based on the theory of moments, considering internal pressure and material nonlinearity, has been developed using the finite difference method. The analysis of the obtained results showed that the meridional stress decreased by 13.6% in the first approximation, 8.74% in the second approximation, and 3.26% in the third approximation, compared to the linear case. The radial displacement accumulation increased by 10.26% in the first approximation, 7.82% in the second approximation, and 3.82% in the third approximation, compared to the linear case.

Based on the developed methodology, a calculation algorithm has been formulated, and the results of the performed calculations are presented in the form of graphs, which allows for their application in engineering practice.

3.3. Nomenclature (symbols and terminology)

As shown in **Table** 1, the symbols and terminology used in this analysis are defined systematically to enhance clarity and ensure consistency throughout the paper.

4. Discussion

The adoption of the elastoplastic model allows for a more precise representation of material behavior under critical loading conditions. This approach, unlike traditional linear models, accounts for both elastic and plastic deformations, providing a deeper understanding of the structural response in real-world applications. The adoption of the elastoplastic model allows for a more precise representation of material behavior under critical loading conditions. Unlike traditional linear models, this approach accounts for both elastic and plastic deformations, offering a deeper understanding of the structural response in real-world applications. An analytical investigation was conducted on the stability of a fluid-conveying tubular element, taking into account the elastoplastic behavior of the material. Analytical relationships were derived to determine critical states and assess the influence of flow velocity on structural stability.

The developed method for calculating and optimizing the geometric parameters of marine hydraulic structure elements, specifically vertical risers under internal pressure, while considering the material's physical nonlinearity, has proven highly effective in addressing practical engineering challenges. The results indicate that the application of nonlinear theory facilitates the identification of additional strength reserves, a refinement of stress and deformation distributions, and optimization of cross-sectional dimensions and shapes.

When compared to conventional thin-shell analysis methods, the proposed approach demonstrates clear advantages in terms of convergence speed and accuracy in predicting the stress-strain state. Furthermore, the method is versatile, applicable to a wide range of structural problems, including shells with constant and variable thicknesses subjected to various external and internal loads. Its ability to accurately capture material nonlinearity and efficiently handle various loading scenarios sets

Table 1. Nomenclature of symbols used in the analysis.

Symbol	Definition	Unit	Application/Comment
1	2	3	4
P_b	Pressure at the upper end (pipe inlet)	Pa	Pressure at the pipe inlet
P_0	Reference pressure	Pa	The pressure at a reference point, often the atmospheric pressure
ρ	Density of the fluid	kg/m^3	Fluid density
ϑ	Fluid velocity	m/s	Fluid velocity in the pipe
P_n	Pressure at the lower end (pipe outlet)	Pa	Pressure at the pipe outlet
P_v	Pressure at the upper end (inlet)	Pa	Pressure at the pipe inlet
P_{sk}	Dynamic head	Pa	Dynamic head, representing the fluid's kinetic energy per unit volume
F_n	Cross-sectional area of the pipe	m^2	Cross-sectional area through which the fluid flows
q	Weight of the fluid per unit length of the pipe	N/m	Weight of the fluid per unit length
g	Acceleration due to gravity	m/s2	Gravitational acceleration, typically 9.81m/s^2
M_x	Bending moment at an arbitrary section	Nm	Bending moment at the given section along the x-axis
M_0	Initial bending moment at the reference point	Nm	Initial bending moment at the reference section
Q_0	Shear force at the reference point	N	Shear force at the reference section
x	Distance from the reference point to the section	m	Distance along the beam from the reference point to the current section
N	Axial force	N	Axial force along the length of the beam
y	Vertical distance from the neutral axis	m	Vertical displacement from the neutral axis
y_0	Vertical distance of the reference point from the neutral axis	m	Vertical displacement at the reference point from the neutral axis
E	Modulus of elasticity	Pa	Material property, representing the stiffness of the material
J	Area moment of inertia	m4	Geometrical property of the rod's cross-section that resists bending
q_0	Distributed load at the reference point	N/m	Load per unit length at the reference point
σ_a	Yield stress of the rod material	Pa (N/m^2)	Stress at which the material begins to plastically deform
c	Height of the compressed zone of the elastic core	m	Height of the compressed zone in the rod's elastic region
e_0	Initial deflection or displacement at reference point	m	Initial deflection or displacement at the reference point
l	Length of the rod	m	Total length of the rod
F	Cross-sectional area of the rod	m^2	Cross-sectional area of the tubular rod
α	Central angle of the section	radians	Angle measured from the vertically downward radius
φ	Boundary angle between elastic core and plastic zone	radians	Angle separating the elastic core from the plastic zone in the rod
σ_1	Maximum stress on the concave side (yield stress)	Pa (N/m^2)	Maximum stress in the concave region of the rod at midsection
σ_2	Stress on the convex side (less than yield stress)	Pa (N/m^2)	Stress in the convex region of the rod at midsection, which is less than σ_a
σ_0	Axial stress	Pa	Tubular rod, critical load calculation
r	Radius of the tubular section	m	Radius of the cross-section of the tubular rod
δ	Small displacement factor	m	Small displacement factor, possibly related to strain or deflection
w	Section modulus of the tubular section	m^3	Section modulus of the tubular section, related to resistance to bending
λ	Flexibility coefficient	-	A dimensionless parameter related to flexibility
ϕ	Angle for the elastic-plastic boundary	radians	Angle representing the boundary of elastic core
ψ	Angle for the start of the plastic zone in the tubular section	radians	Angle marking the beginning of the plastic deformation zone
λ^2	Flexibility parameter for the tubular rod in equilibrium	-	Flexibility parameter for the tubular rod in equilibrium
π	Mathematical constant	-	Constant used in circular and angular calculations
1	2	3	4
$\Theta(\varphi, \psi)$	Stability function	-	Function used to determine the critical state of the rod under stress and bending. Specifically, it describes the equilibrium condition for the stress

Table 2. (*Continued*)

Symbol	Definition	Unit	Application/Comment
T_x	Longitudinal normal force	N/m	Force in the shell's cross-section along the pipe's length
T_t	Tangential normal force	N/m	Force in the shell's cross-section perpendicular to the length
h	Pipe wall thickness	m	Pipe wall thickness
P_1, P_2	Meridian and tangential projections of forces	N	Meridian and tangential projections of forces
u	Axial displacement	m	Displacement along the axis of the pipe
w	Radial displacement	m	Displacement perpendicular to the pipe's axis.
μ	Poisson's ratio	-	Material constant describing the ratio of lateral strain to axial strain
β	Nonlinear constant	-	Constant related to the nonlinear stress-strain behavior of the material
ϵ_x, ϵ_y	Relative and angular deformations	-	Deformations in the pipe due to applied forces
D	Flexural rigidity	N·m^2	Flexural rigidity of the shell
M_x	Longitudinal bending moment	N·m	Bending moment acting in the longitudinal direction of the pipe due to internal pressure and displacement.
M_t	Tangential bending moment	N·m	Bending moment acting in the tangential direction of the pipe due to internal pressure and displacement.
x	Axial coordinate	m	Position along the length of the pipe.
σ_x	Longitudinal stress	Pa	Stress acting along the axial direction of the pipe (or rod), caused by internal pressure or external force
σ_y	Radial stress	Pa	Stress acting in the radial direction of the pipe (or rod), typically associated with internal pressure or external loads
z	Coordinate in the longitudinal direction	m	Longitudinal coordinate along the pipe or rod, used to define the position along the structure.
ν	Small parameter	-	Represents the ratio of the nonlinear behavior to the material's linear elasticity.
ϵ_0	Relative linear deformation	-	The deformation corresponding to the material's strength limit.
γ_0	Angular deformation	-	Angular deformation corresponding to the material's ultimate strength.
T_{x_0}	Normal force in the shell's cross-section, axial direction	N/m	Initial normal force in axial direction at j=0
T_{t_0}	Tangential force in the shell's cross-section	N/m	Initial tangential force at j=0
M_{x_0}	Bending moment in the shell at j=0	N·m	Initial bending moment at j=0
M_{t_0}	Tangential bending moment in the shell at j=0	N·m	Initial tangential moment at j=0
T_{x_1}	Normal force in the shell's cross-section, axial direction at j=1	N/m	Normal force after considering nonlinearity
T_{t_1}	Tangential force in the shell's cross-section at j=1	N/m	Tangential force after considering nonlinearity
M_{x_1}	Bending moment in the shell at j=1	N/m	Bending moment after considering nonlinear effects
M_{t1}	Tangential bending moment in the shell at j=1	N/m	Tangential moment after considering nonlinear effects
T_{x_2}	Normal force in the shell's cross-section, axial direction at j=2	N/m	Normal force for the second term in the series expansion
T_{t_2}	Tangential force in the shell's cross-section at j=2	N/m	Tangential force for the second term in the series expansion
M_{x_2}	Bending moment in the shell at j=2	N/m	Bending moment for the second term in the series expansion
M_{t_2}	Tangential bending moment in the shell at j=2	N/m	Tangential moment for the second term in the series expansion
ω_0	Displacement at j=0	m	Displacement at the first term in the series expansion
ω_1	Displacement at j=1	m	Displacement at the second term in the series expansion
ω_2	Displacement at j=2	m	Displacement at the third term in the series expansion

it apart from traditional methods. This advantage is especially noticeable when analyzing large-scale offshore structures, where traditional approaches may fail to predict failure modes and stress distributions with the required precision.

The practical significance of this study lies in the application of the derived formulas and recom-

mendations to the design and analysis of marine hydraulic structures, thereby enhancing both reliability and manufacturability. A limitation of the method is its reliance on the accurate specification of material properties and element geometry, requiring reliable experimental data. Nevertheless, the analysis of the results clearly demonstrates that accounting for material nonlinearity in stress determination leads to a more accurate definition of the stress-strain state, ensuring the robustness and safety of offshore structures.

5. Conclusion

This study has developed a method for calculating and optimizing the geometric parameters of elements in marine hydraulic structures, specifically vertical risers subjected to internal pressure, while accounting for material physical nonlinearity. The results demonstrate the method's ability to accurately predict the stress-strain state, identify additional strength reserves, and optimize the shapes and dimensions of structural elements.

The proposed method exhibits both high accuracy and rapid convergence, making it suitable for a broad range of nonlinear structural mechanics problems. Its practical significance is evident in the ability to apply the derived formulas and recommendations in the design and analysis of marine hydraulic structures, thereby enhancing both reliability and manufacturability.

Furthermore, the stress-strain relationship in a vertical pipe under internal fluid flow has been analyzed using nonlinear theory, and the findings are presented in the Graphical Abstract.

5.1. Future research directions

The methodology provides a robust framework for further studies. Future work could focus on the refinement of material models, expansion to more complex engineering scenarios, integration with other offshore structural components, and iterative improvement of analytical and numerical techniques. These directions ensure that the method remains applicable and adaptable for subsequent research in the field of offshore hydraulic structures.

Additionally, while fractional derivatives were not used in this study, it is emphasized that they are becoming an important tool in modern research. These derivatives offer new analytical perspectives for modeling complex physical systems and are increasingly applied in various fields such as engineering, physics, and applied mathematics. In these areas, fractional derivatives provide significant contributions to both the development of analytical methods and computational approaches and could be used for modeling nonlinear material behavior and analyzing complex structures.

Acknowledgments

None.

Funding

None.

Conflict of interest

The authors declare they have no competing interests.

Author contributions

Conceptualization: All authors
Investigation: All authors
Methodology: All authors
Writing – original draft: Latif F. Aslanov
Writing – review & editing: Ulvi L. Aslanli

Availability of data

Not applicable.

AI tools statement

All authors confirm that no AI tools were used in the preparation of this manuscript.

References

1. Al-Kwradi M, Altarawneh M. Degradation pathways of amino acids during thermal utilization of biomass: a review. *Front Chem Sci Eng.* 2024;18:78. https://www.doi.org/10.1007/s11705-024-2433-1
2. Alam S, Manzur T, Matthews J, et al. Experimental and analytical investigation on friction resistance force between buried coated pressurized steel pipes and soil. *Front Struct Civ Eng.* 2024;18:615-629. https://www.doi.org/10.1007/s11709-024-1017-y
3. Arroussi C, Belalia A, & Meliani MH. Temperature effects on the resistance capacity of API X60 pipe elbow under bending moment using X-FEM method. *J Mech Sci Technol.* 2024;38:661-669. https://www.doi.org/10.1007/s12206-024-0114-0
4. Arun Sundaram B, Kesavan K, & Parivallal S. Recent Advances in Health Monitoring and Assessment of In-service Oil and Gas Buried Pipelines. *J Inst Eng India Ser.* 2018;99:729-740.

https://www.doi.org/10.1007/s40030-018-0316-5

5. Asif R, Lee HW, & Hu JW. Oil plant piping structure multi-factor optimization approach for enhancing fatigue life using one-way FSI analysis. *J Mech Sci Technol.* 2025;39:4027-4042. https://www.doi.org/10.1007/s12206-025-0627-1
6. Aslanov LF. Wave interaction of offshore structure and shelf soil through large section piles with a 'hard core' on the half-space model. *Neft khozyaystvo.* 2015a;(2):78-81. https://www.researchgate.net/publication/286035701_Wave_interaction_of_offshore_structure_and_shelf_subgrade_through_the_large_cross-section_pile_with_rigid_core_along_the_model_of_semispace
7. Aslanov LF. Interaction between large cross-sections bored piles with 'hard core' under dynamic loads and shelf soils. *Sci Bull Natl Min Univ.* 2015b;(5):21-25. http://irbis-nbuv.gov.ua/cgi-bin/irbis_nbuv/cgiirbis_64.exe?C21COM=2&I21DBN=UJRN&P21DBN=UJRN&IMAGE_FILE_DOWNLOAD=1&Image_file_name=PDF/Nvngu_2015_5_5.pdf
8. Aslanov LF. "Reflected waves from bored or CFA piles of large section in the offshore soils. *Neft khozyaystvo.* 2016;7:112-116. https://www.researchgate.net/publication/318492911_Reflected_waves_from_bored_or_CFA_piles_of_large_section_in_the_offshore_soils
9. Aslanov LF. Optimization of the Calculation of the Piles of Fixed Offshore Platforms. In: El-Askary H, Erguler ZA, Karakus M0, Chaminé, H.I. (eds) Research De-velopments in Geotechnics, Geo-Informatics and Remote Sensing. CAJG 2019. *Advances in Science Technology & Innovation.* Springer, Cham. 2022. https://www.doi.org/10.1007/978-3-030-72896-0_32
10. Aslanov LF, Aslanli UL. Study of the stress-strain state of the pontoon element of the support block. *SOCAR Proceedings.* 2024a;2:115-121. http://dx.doi.org/10.5510/OGP20240200976
11. Aslanov LF, Aslanli UL. Study of Marine Hydraulic Structures Under Seismic Effects. In: Ksibi M, et al. Recent Advances in Environmental Science from the Euro-Mediterranean and Surrounding Regions (4th Edition). EMCEI 2022. *Advances in Science Technology & Innovation.* Springer, Cham. 2024b. https://www.doi.org/10.1007/978-3-031-51904-8_193
12. Aslanov LF, Aslanli UL. Determination of load-bearing capacity of piles used in stationary offshore platforms. *SOCAR Proceedings.* 2024c;1:116-123. http://dx.doi.org/10.5510/OGP240100949
13. Aslanov LF, Aslanov FL. Choosing an Effective Design Solution for Fixing Offshore Hydro-Technical Structures to Shelf Ground. In: Çiner A, et al. Recent Research on Geotechnical Engineering, Remote Sensing, Geophysics and Earthquake Seismology. MedGU 2021. *Advances in Science Technology & Innovation.* Springer, Cham. 2024a. https://www.doi.org/10.1007/978-3-031-43218-7_22
14. Aslanov LF, Aslanov FL. Some Tasks of Increasing and Identifying the Reserves of the Bearing Capacity of Anchor Fastenings of Offshore Fixed Platforms. In: Bezzeghoud M, et al. Recent Research on Geotechnical Engineering, Remote Sensing, Geophysics and Earthquake Seismology. MedGU 2022. *Advances in Science Technology & Innovation.* Springer, Cham. 2024b. https://www.doi.org/10.1007/978-3-031-48715-6_10
15. Aslanov LF, Aslanli UL, Aslanov FL. Construction of foundations for reservoirs in the Caspian Sea. *SOCAR Proceedings.* 2024;(1):29-38. http://dx.doi.org/10.5510/OGP2024SI101031
16. Aslanov LF, Aslanli UL, Aslanov FL. New calculation method for the pontoon element of offshore fixed platforms for oil and gas production. *Nafta-Gaz* 2025;3:188-198. https://www.doi.org/10.18668/NG.2025.03.05
17. Aslanov LF, Aslanov FL. Local Stability of Elements from Sealed Pipes of Fixed Offshore Platforms. In: Çiner A, et al. Recent Research on Sedimentology, Stratigraphy, Paleontology, Tectonics, Geochemistry, Volcanology and Petroleum Geology. MedGU 2023. *Advances in Science Technology & Innovation.* Springer, Cham. 2025. https://www.doi.org/10.1007/978-3-031-87558-8_38
18. Aslanov LF, & Aslanli UL. A methodology for calculating the load-bearing capacity of pile foundations in offshore hydraulic structures based on principles of rational design. An *International Journal of Optimization and Control: Theories & Applications.* 2026;16(1):138-159. https://www.doi.org/10.36922/IJOCTA025340146
19. Bochkarev SV, Galinovskii AL. & Salnikov AF. A Vibroacoustic Method for Diagnosing the Influence of Impulse Load on Fiberglass Pipes. *Polym Sci Ser.* 2022;15:652-657. https://www.doi.org/10.1134/S1995421222040025
20. Carloni ACN, Conde KEd, Pantaleão AV, et al. Validation and analysis of turbulence modeling in pipe elbow under secondary flow conditions. *J Braz Soc Mech Sci Eng.* 2022;44:595. https://www.doi.org/10.1007/s40430-022-03899-9
21. Chen H, Cui J, Li Y, et al. (2025) Influence of Internal Water on Dynamic Response of Underground Pipelines. *Soil Mech Found Eng.* 2025;62:348-356. https://www.doi.org/10.1007/s11204-025-10067-3

22. Chen W, Cao Y, Guo X, et al. Nonlinear vibration analysis of pipeline considering the effects of soft nonlinear clamp. *Appl Math Mech-Engl Ed.* 2022;43:1555-1568. https://www.doi.org/10.1007/s10483-022-2903-7
23. Chen W, Qu X, Zhang R, et al. Nonlinear stress analysis of aero-engine pipeline based on semi-analytical method. *Appl Math Mech-Engl Ed.* 2025;46:521-538. https://www.doi.org/10.1007/s10483-025-3225-8
24. Chinchanikar S, Mulik H, Varude P, et al. A review of emerging hydroforming technologies: design considerations, parametric studies, and recent innovations. *J Eng Appl Sci.* 2024;71:205. https://www.doi.org/10.1186/s44147-024-00546-z
25. Da Silva DL, Echer L, Rojo Tanzi BN, et al. Experimental investigation of the structural performance of fiber-reinforced patches in the repair of locally damaged steel pipes. *J Braz Soc Mech Sci Eng.* 2023;45:435. https://www.doi.org/10.1007/s40430-023-04348-x
26. Du X, Li Z, Fang H, et al. Numerical and practical investigation of the multiple hole grouting repair law of underground drainage pipeline defects. *Bull Eng Geol Environ.* 2023;82:44. https://www.doi.org/10.1007/s10064-023-03070-1
27. Eipakchi H, Nasrekani FM, & Ahmadi S. An analytical approach for the vibration behavior of viscoelastic cylindrical shells under internal moving pressure. *Acta Mech.* 2020;231:3405-3418. https://www.doi.org/10.1007/s00707-020-02719-2
28. Fan H, Xie Y, & Wang Q. Stress-strain model of austenitic stainless steel for pressure vessel design. *J Mech Sci Technol.* 2023;37:481-3494. https://www.doi.org/10.1007/s12206-023-0613-4
29. Fu C, Quan L, Geng Y, et al. (2025) Dynamic response of reinforced soft tubes: A numerical and experimental investigation. *J Mech Sci Technol.* 2025;39:3883-3896. https://www.doi.org/10.1007/s12206-025-0612-8
30. Gan Cb, Guo Sq, Lei H, et al. Random uncertainty modeling and vibration analysis of a straight pipe conveying fluid. *Nonlinear Dyn.* 2014;77:503-519. https://www.doi.org/10.1007/s11071-014-1313-5
31. Gholami M, Eftekhari M. Nonlinear forced vibration in a subcritical regime of a porous functionally graded pipe conveying fluid with a retaining clip. *Appl Math Mech-Engl Ed.* 2025;46:101-122. https://www.doi.org/10.1007/s10483-025-3206-9
32. Guo J, Zhang Y, Cheng Y, et al. Study on urban ground collapse induced by defective pipelines based on physical model experiments and numerical simulation. *Sci Rep.* 2025;15:6085. https://www.doi.org/10.1038/s41598-025-90146-5
33. Guo X, Liu Q, Han X, et al. High-precision numerical modeling of the projectile launch and failure mechanism analysis of projectile-borne components. *Appl Math Mech-Engl Ed.* 2025;46:885-906. https://www.doi.org/10.1007/s10483-025-3254-9
34. Hajiyev MA, Huseynov IG, Hajiyeva UM, Alaeva SM. Calculation of metal elements deflection using a three-line strain diagram. *SOCAR Proceedings.* 2024;2:109-114. https://www.doi.org/10.5510/OGP20240200975
35. Hernández-Rojo MA, Alamilla-Lopez JL, Dominguez-Aguilar MA, et al. Experimental and numerical analysis of failure in flexible pipe by a mechanism of intentional damage. *J Mech Sci Technol.* 2020;34:1979-1988. https://www.doi.org/10.1007/s12206-020-0419-6
36. Huang M, Qian X, Xu J, et al. Evaluation of the submarine debris-flow hazard risks to planned subsea pipeline systems: a case study in the Qiongdongnan Basin, South China Sea. *Acta Oceanol Sin.* 2023;42:139-153. https://www.doi.org/10.1007/s13131-022-2123-0
37. Iskandarov EKh, Ismayilova FB, Shukurlu MF, Ismayilova PSh. Changes in energy characteristics of pipeline systems considering hydrodynamic loads. *SOCAR Proceedings.* 2024;(2):105-108. https://www.doi.org/10.5510/OGP20240200974
38. Iskandarov EKh. STUDY OF STRUCTURAL CHANGES IN MULTIFACETED GAS PIPELINES. *SOCAR Proceedings.* 2024;(4):117-122. https://www.doi.org/10.5510/OGP20240401026
39. Ji L, Li Y, Li W, et al. Investigation of vortex dynamics diagnosis in the stall state of mixed-flow pump with blade gap size effect. *J Braz Soc Mech Sci Eng.* 2023;45:395. https://www.doi.org/10.1007/s40430-023-04268-w
40. Jones JF, Raj V, Abas PE, et al. Application of artificial intelligence for asset integrity management of offshore oil and gas pipelines. *Life Cycle Reliab Saf Eng.* 2025.

https://www.doi.org/10.1007/s41872-025-00353-2

41. Kandil M, El-Sayed TA, & Kamal AM. Unveiling the impact of pipe materials on water hammer in pressure pipelines: an experimental and numerical study. *Sci Rep.* 2024;14:30599. https://www.doi.org/10.1038/s41598-024-80853-w
42. Khan M, Khan N, Ullah I, Shah K, Abdeljawad T, & Abdalla BA. A novel fractal fractional mathematical model for HIV/AIDS transmission stability and sensitivity with numerical analysis. *Scientific Reports.* 2025;15(1):23. https://www.doi.org/10.1038/s41598-025-93436-0
43. Kovtun AV, Tabunenko VO, Nesterenko S, et al. Determining the Strength of Tanks with Fluid in the Case of Free Dropping. *Int Appl Mech.* 2023;59:107-113. https://www.doi.org/10.1007/s10778-023-01204-2
44. Kubenko VD, Koval'chuk PS. Stability and Nonlinear Vibrations of Closed Cylindrical Shells Interacting with a Fluid Flow (Review). *Int Appl Mech.* 2015;51:12-63. https://www.doi.org/10.1007/s10778-015-0672-z
45. Lee Y, Lee ET. Analysis of prestressed concrete cylinder pipes with fiber reinforced polymer. *KSCE J Civ Eng.* 2015;19:682-688. https://www.doi.org/10.1007/s12205-013-0006-9
46. Lu P, Sheng X, Gao Y, et al. Influence of Shear Effects on the Characteristics of Axisymmetric Wave Propagation in a Buried Fluid-Filled Pipe. *Chin J Mech Eng.* 2022;35:74. https://www.doi.org/10.1186/s10033-022-00710-7
47. Lu W, Li Z, Tang X, et al. Effects of Operation Parameters on Heat Transfer in Tubular Moving Bed Heat Exchangers: A CFD-DEM Study. *J Therm Sci.* 2025;34:542-554. https://www.doi.org/10.1007/s11630-024-2063-4
48. Luan Y, Zhuang Y, Wang G et al. Deformation behavior in the tube hydro-pressing of rectangular cross-section components. *Int J Adv Manuf Technol.* 2025;138:4561-4575. https://www.doi.org/10.1007/s00170-025-15751-0
49. Li F, An C, Duan M, et al. In-plane and out-of-plane dynamics of curved pipes conveying fluid by integral transform method. *J Braz Soc Mech Sci Eng.* 2019;41:542. https://www.doi.org/10.1007/s40430-019-2053-8
50. Li G, Liu G, Wang H, et al. Throttle valve erosion in the oil and gas industry. *J Mater Sci.* 2024;59:20874-20899. https://www.doi.org/10.1007/s10853-024-10334-y
51. Li P, Zhang Z, Wang W, et al. Vibration Manipulation Properties of Phononic Crystals and Acoustic Metamaterials for Fluid-Conveying Pipeline Systems: A Review. *J Vib Eng Technol.* 2025;13:114. https://www.doi.org/10.1007/s42417-024-01673-w
52. Lin J, Li Z, Ning Z, et al. On the mechanism of the post buckling and the initiation of a propagating buckle in sandwich pipelines based on shear deformation theory. *J Mech Sci Technol.* 2025;39:777-793. https://www.doi.org/10.1007/s12206-025-0122-8
53. List A, Huang C, Wiehler L, et al. Influence of Ductility on Fracture in Tensile Testing of Cold Gas Sprayed Deposits. *J Therm Spray Tech.* 2023;32:1780-1795. https://www.doi.org/10.1007/s11666-023-01598-y
54. Liu Hl, Hou C, Li L, et al. Experimental investigation on flow properties of cemented paste backfill through L-pipe and loop-pipe tests. *J Cent South Univ.* 2021;28:2830-2842. https://www.doi.org/10.1007/s11771-021-4810-y
55. Mao X, Ding H, & Chen L. Bending vibration control of pipes conveying fluids by nonlinear torsional absorbers at the boundary. *Sci China Technol Sci.* 2021;64:1690-1704. https://www.doi.org/10.1007/s11431-020-1791-2
56. Okolie O, Latto J, Faisal N, et al. Manufacturing Defects in Thermoplastic Composite Pipes and Their Effect on the in-situ Performance of Thermoplastic Composite Pipes in Oil and Gas Applications. *Appl Compos Mater.* 2023;30:231-306. https://www.doi.org/10.1007/s10443-022-10066-9
57. Orjiocha SI, Eze FC, Salem MAS, et al. Plant-derived extracts for mitigating scale formation in pipelines and industrial sys-

tems: a review of status. *Discov Mater.* 2025;5:201. https://www.doi.org/10.1007/s43939-025-00365-w

58. Orynyak IV, Dubyk YR, & Batura AS. Analysis of Fluid-Induced Vibrations of Long Branched Pipelines. *Strength Mater.* 2015;47:314-331. https://www.doi.org/10.1007/s11223-015-9661-z
59. Pacheco A, Viotti M, Veiga CN, et al. Evaluation of Bending Stresses in Pipelines by Using Hole-drilling Measurements Combined with Interferometry. *Exp Mech.* 2016;56:133-143. https://www.doi.org/10.1007/s11340-015-0079-0
60. Parviz M, Aminnejad B, & Fiouz A. Numerical simulation of dynamic response of water in buried pipeline under explosion. *KSCE J Civ Eng.* 2017;21:2798-2806. https://www.doi.org/10.1007/s12205-017-0889-y
61. Plasencia J, Inkson N, & Nydal OJ. Research on the viscosity of stabilized emulsions in different pipe diameters using pressure drop and phase inversion. *Exp Comput Multiph Flow.* 2022;4:241-263. https://www.doi.org/10.1007/s42757-020-0102-2
62. Rajabiani E, Gharib MR, & Koochi A. Buckling Analysis of Groove Corroded Pipe Due to Axial Pressure with Finite Element Method. *Int J Steel Struct.* 2021;21:1723-1740. https://www.doi.org/10.1007/s13296-021-00531-9
63. Rao Y, Wang Y, Wang S, et al. Numerical simulation study on the influence of bend diameter rate on the flow characteristics of nature gas hydrate particles. *Sci Rep.* 2024;14:31604. https://www.doi.org/10.1038/s41598-024-77890-w
64. Ren J, Zhao Y, Zhang X, et al. Design of a Deformable Pipeline for Efficient Recovery of Protective Coal Pillars. *Rock Mech Rock Eng.* 2025. https://www.doi.org/10.1007/s00603-025-04811-2
65. Seyfipour I, Mirghaderi R, & Bahaari MR. Buckling and stability of subsea HP/HT pipelines on laterally sloping seabeds. *J Ocean Eng Mar Energy.* 2023;9:1-23. https://www.doi.org/10.1007/s40722-022-00245-y
66. Shah K, Abdeljawad T, Abdalla B, et al. Analyzing a coupled dynamical system of materials recycling in chemostat systems with artificial deep neural network. *Model Earth Syst Environ.* 2025;11:313. https://www.doi.org/10.1007/s40808-025-02473-1
67. Sher M, Shah K, Ali Z, & Abdeljawad T. Using deep neural network in computational analysis of coupled systems of fractional integro-differential equations. *J Comput Appl Math.* 2025;474:116912. https://www.doi.org/10.1016/j.cam.2025.116912
68. Shishesaz M, Gatea AH, Moradi S, et al. Stress analysis in the buried polyethylene pipes with viscoelastic behavior: a finite element study. *Discov Appl Sci.* 2024;6:616. https://www.doi.org/10.1007/s42452-024-06331-0
69. Singh J, Gill HS, & Vasudev H. Computational fluid dynamics analysis on role of particulate shape and size in erosion of pipe bends. *Int J Interact Des Manuf.* 2023;17:2631-2646. https://www.doi.org/10.1007/s12008-022-01094-7
70. Song S, Liu G, He S, et al. Study on the gas flow resistance state in unstable collapse boreholes and the classification of borehole types. *Sci Rep.* 2025;15:14433. https://www.doi.org/10.1038/s41598-025-99387-w
71. Sun W, Wu J, Su S-F, & Zhao X. Neural network-based fixed-time tracking control for input-quantized nonlinear systems with actuator faults. *IEEE Transactions on Neural Networks and Learning Systems.* 2024;35(3):3978-3988. https://www.doi.org/10.1109/TNNLS.2022.3201504
72. Sun Z, Yu R, Wang X, et al. Dynamic analysis of liquid-filled clamp-pipe systems based on the spectral element method. *Arch Appl Mech.* 2025;95:24. https://www.doi.org/10.1007/s00419-024-02723-1
73. Tang Y, Zhang HJ, Chen LQ, et al. Recent progress on dynamics and control of pipes conveying fluid. *Nonlinear Dyn.* 2025;113:6253-6315. https://www.doi.org/10.1007/s11071-024-10486-1
74. Valli J, Majumder M, Venkatraman S, et al. Numerical study of pipe-soil interaction under lateral movements on different types of

seabed conditions. *J Ocean Eng Mar Energy.* 2025.
https://www.doi.org/10.1007/s40722-025-00434-5

75. Wang Py, Wan Gh, Wang Zj, et al. Investigation on the stress-strain rate curve of MR fluids in a combined mode and its application in sheet flexible-die forming. *Int J Adv Manuf Technol.* 2021;117:67-79.
https://www.doi.org/10.1007/s00170-021-07301-1
76. Wang My, Yao Hy, Liu Yf, et al. Understanding and probing progression of localized corrosion on inner walls of steel pipelines: an overview. *J Iron Steel Res Int.* 2025;32:1–18.
https://www.doi.org/10.1007/s42243-024-01213-6
77. Wang ZY, Liu JC, Tan Y, et al. Experimental and numerical investigation on internal erosion induced by infiltration of defective buried pipe. *Bull Eng Geol Environ.* 2025;84:38.
https://www.doi.org/10.1007/s10064-024-04073-2
78. Wu HG, Yu JH, Shi CZ, et al. Pipe-Soil Interaction and Sensitivity Study of Large-Diameter Buried Steel Pipes. *KSCE J Civ Eng.* 2021;25:793-804.
https://www.doi.org/10.1007/s12205-021-0392-3
79. Wu T, Yu H, Jiang N, et al. Theoretical analysis of the deformation for steel gas pipes taking into account shear effects under surface explosion loads. *Sci Rep.* 2022;12:8658.
https://www.doi.org/10.1038/s41598-022-12698-0
80. Yeganeh M, Heydarie Y, Shahryari Z, et al. Corrosion Inhibitor of API Pipeline Steels: A Review. *J Bio Tribo Corros.* 2025;11:44.
https://www.doi.org/10.1007/s40735-025-00965-2
81. Xue X, Zhu J, & Sang Z. Study on design pressure of in-service welding pipes. *SCI CHINA SER E.* 2006;49:434-444.
https://www.doi.org/10.1007/s11431-006-2005-2
82. Yu C, Guo Z, Pan Z, et al. Performance and Stress Analysis of Flat-Tubular Solid Oxide Fuel Cells Fueled with Methane and Hydrogen. *Acta Mech Solida Sin.* 2025;38:402-414.
https://www.doi.org/10.1007/s10338-024-00514-3
83. Yu J, Wu M, Sun Z, et al. Research progress of buckling propagation experiment of deepwater pipelines. *Trans Tianjin Univ.* 2016;22:285-293.
https://www.doi.org/10.1007/s12209-016-2801-0
84. Yu J, An C, Zhang Y, et al. Experimental and Numerical Study on Vortex-Induced Vibration Suppression by Helical Strakes on Subsea Pipelines. *J Marine Sci Appl.* 2025;24: 580-592.
https://www.doi.org/10.1007/s11804-025-00650-3
85. Yuan J, Sun W, Sun Y, & Su S-F. Mask privacy preservation prescribed-time consensus control for nonlinear multi-agent systems. *IEEE Trans Autom Sci Eng.* 2025;22:11554-11563.
https://www.doi.org/10.1109/TASE.2025.3535924
86. Yue C, Ma Q, Yang Z, et al. Multi-jointed pneumatic sealing disc of fluid-driven pipeline robot: impacts of structural parameters on performance. *J Braz Soc Mech Sci Eng.* 2024;46:80.
https://www.doi.org/10.1007/s40430-023-04655-3
87. Zangeneh S. Fitness-for-Service Assessment of Local Thin Area in a Line Pipe. *J Fail Anal & Preven.* 2021;21:1085-1095.
https://www.doi.org/10.1007/s11668-021-01161-3
88. Zeng D, Luo J, Ke R, et al. Research Progress on Tribo-Corrosion Behavior of Oil Country Tubular Goods: A Review. *J Bio Tribo Corros.* 2025;11:122.
https://www.doi.org/10.1007/s40735-025-01048-y
89. Zhang H, Li Y, Xu Z, et al. Modal analysis of PE pipeline under seabed dynamic pressure. *Sci Rep.* 2024;14:29198.
https://www.doi.org/10.1038/s41598-024-80583-z
90. Zhang H, Zhang J, Lin R, Wang Y. Damage Mechanism Investigation of Offshore Pipelines Impacted by Falling Objects. In: Submarine Pipeline Integrity: Assessment of Failure Modes and Advanced Evaluation Techniques. *Ocean Engineering & Oceanography.* Springer, Cham. 2025;28.
https://www.doi.org/10.1007/978-3-031-92092-9_3
91. Zhang W, Sun W, Yuan W, et al. Progress and prospect of particle finite element method for large deformation simulation in geotechnical engineering. *Comp Part Mech.* 2025;12:1893-1911.

https://www.doi.org/10.1007/s40571-025-01000-4

92. Zhao D, Liu J, & Wu CQ. Stability and local bifurcation of parameter-excited vibration of pipes conveying pulsating fluid under thermal loading. *Appl Math Mech-Engl Ed.* 2015;36:1017-1032. https://www.doi.org/10.1007/s10483-015-1960-7

Prof. Dr. Latif F. Aslanov *has over 30 years of experience at the "Oil-Gas" Research Project Institute of SOCAR, where he has held positions including Research Associate, Leading Research Associate, Head of the Laboratory of Marine Hydrotechnical Installations, and Head of the Technical Production Department. He is also an Associate Professor at the Azerbaijan University of Architecture and Construction. His research focuses on the strength, stability, durability, and operational resources of marine hydrotechnical oil and gas mining structures, including long-length driven piles and platform structures under static and dynamic loads. Prof. Aslanov has contributed to several widely applied normative documents and conducted extensive experimental investigations on hydrotechnical objects and large-scale models.*

https://orcid.org/0000-0003-1546-5436

Ulvi L. Aslanli *is a lecturer in the Department of Foundations and Underground Structures at Azerbaijan Structural and Architectural University and a senior structural engineer at SOCAR. With over eight years of academic and industry experience in construction engineering, he specializes in geotechnical engineering, soil mechanics, structural software, and foundation engineering. Ulvi holds a Master's degree in Construction Engineering and Management and is pursuing a Ph.D. on the stress–strain state of marine hydraulic structures. He has authored several peer-reviewed papers and works closely with industry professionals to connect theory and practice.*

https://orcid.org/0009-0001-1504-5258

An International Journal of Optimization and Control: Theories & Applications (https://accscience.com/journal/ijocta)